Inorg. Chem. **2004**, *43*, 5311–5320

Studies on Reactions INCX → IXCN (X = O, S, and Se)

Yanli Zeng,[†,‡] Shijun Zheng,*[,†,‡] and Lingpeng Meng[‡]

Department of Chemistry, Graduate School, Chinese Academy of Sciences, Beijing 100039, P. R. China, and Institute of Computational Quantum Chemistry, College of Chemistry, Hebei Normal University, Shijiazhuang 050091, P. R. China

Received March 23, 2004

The reactions of INCO to IOCN, INCS to ISCN, and INCSe to ISeCN have been studied at the MP2/6-311++G-(2df)//B3LYP/6-311++G(2df) level. Geometries of reactants, transition states, and products have been optimized, and geometries of transition states are reported for the first time. The reasons that INCO, ISCN, and ISeCN are easily detected instead of IOCN, INCS, and INCSe have been explained successfully. The breakage and formation of chemical bonds along the reaction paths have been discussed by the topological analysis method of electronic density. The calculated results show that there are two kinds of structure transition states (STS) in the reactions studied.

1. Introduction

Many textbooks and articles do not distinguish between molecular structure and molecular geometry. The theory of atoms in molecules (AIM) defines structure as distinct from geometry using the topology of the electron density, thereby avoiding the confusion that can arise when the two concepts are used interchangeably.[1−6] Judging the breakage or formation of a bond is almost impossible with experimental methods and traditional population analysis. Topological studies on reaction paths of some typical reactions have been carried out by some authors in recent years,[1−9] but much more is still to be known about the relationship between the topological characteristics of density distribution and the energy variation along the reaction path.

For the series of molecules that contains OCN, SCN, and SeCN fragments, a complication that arises is that the remaining group can, in principle, be bonded to both ends of the fragment. Pure INCO, ISCN, and ISeCN have been prepared in the HeI photoelectron spectrometer (PES) by heterogeneous reactions of ICl gas with AgNCO and AgSCN at room temperature and AgSeCN at −9 ±1 °C, respectively.[10] From the PES study of the compounds INCO, ISCN, and ISeCN,[10−12] it has been shown that in these cases the iodine atom is bonded only to N for the NCO group, to S for the NCS group, and to Se for the NCSe group. No signals of IOCN, INCS, or INCSe were obtained.

To explain the reason that the iodine atom is bonded to the OCN group through N, to the SCN group through S and to the SeCN group through Se, we carried out studies on the reactions of INCX → IXCN (X = O, S, and Se). The geometries of the energy transition states of the three reactions are reported for the first time. The breakage and formation of the bonds in the isomerization reaction paths have been discussed, and the structure transition states of the titled reactions are found. This paper is an extension and an additional example of the established ideas and concepts of AIM.[1−5]

* Author to whom correspondence should be addressed. E-mail: sjzheng@mail.hebtu.edu.cn.
† Chinese Academy of Sciences.
‡ Hebei Normal University.

(1) Bader, R. F. W.; Nguyen-Dang, T. T.; Tal, Y. *J. Chem. Phys.* **1979**, *70*, 4316.
(2) Tal, Y.; Bader, R. F. W.; Nguyen-Dang, T. T. *J. Chem. Phys.* **1981**, *74*, 5162.
(3) Bader, R. F. W.; Nguyen-Dang, T. T.; Tal, Y. *Rep. Prog. Phys.* **1981**, *44*, 893.
(4) Bader, R. F. W. *Atoms in Molecules: A Quantum Theory*; Clarendon Press: Oxford, U.K., 1990.
(5) Bader, R. F. W.; Tang, T.-H.; Tal, Y. Biegler-König F. W. *J. Am. Chem. Soc.* **1982**, *104*, 946.
(6) Popelier, P. *Atoms in Molecules: An Introduction*; UMIST: Manchester, U.K. 2000.
(7) Vyboishchikov S. F.; Masunov, A. E. *J. Mol. Struct.: THEOCHEM* **1994**, *311*, 161.
(8) Alikhani, M. E. *Chem. Phys. Lett.* **1997**, *277*, 239.
(9) Dixon, R. E.; Streitwieser A.; Laidig, K. E.; Bader, R. F. W.; Harder S. *J. Phys. Chem.* **1993**, *97*, 3728.
(10) Li, Y. M.; Qiao, Z. M.; Sun, Q.; Zhao, J. C.; Li, H. Y.; Wang, D. X. *Inorg. Chem.* **2003**, *42*, 8846.
(11) Frost, D. C.; MacDonald, C. B.; McDowell, C. A.; Westwood, N. P. C. *Chem. Phys.* **1980**, *47*, 111.
(12) Leung, H.; Suffolk, R. J.; Watts, J. D. *Chem. Phys.* **1986**, *109*, 289.

10.1021/ic0496121 CCC: $27.50
Published on Web 07/24/2004

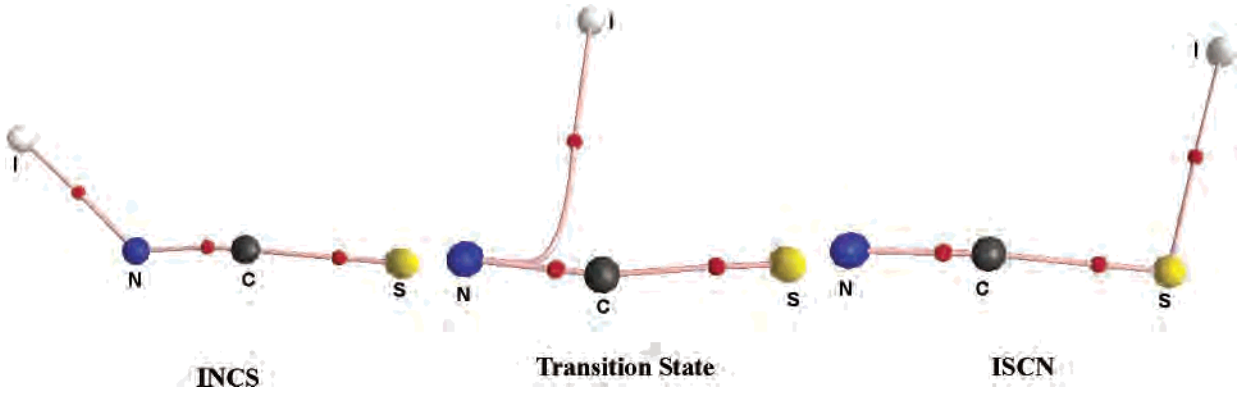

Figure 1. Displays of structures of INCS and ISCN and their transition states. Bond critical points are shown as small spherea.

2. Computational Methods

The geometries of reactants, transition states, products, and every point on the potential energy surface were located by B3LYP calculations with second-order MP2 energy corrections. The 6-311++G(2df) basis set was used for elements N, C, O, S, and Se, and the basis set used for element I was taken from ref 13. The d polar functions were split into $\alpha_1(d_{polar}) = 0.604$ and $\alpha_2(d_{polar}) = 0.151$ by us. The reaction path has been followed using Fukui's theory of the intrinsic reaction coordinate (IRC) method[14] in mass-weighted internal coordinates going in forward and reverse directions from the transition state with the step size equal to 0.01 (amu)$^{1/2}$ bohr. The computations were performed using the Gaussian 98 program.[15] Topological analyses were carried out with the GTA-91 program, which we developed and registered at QCPE (registry number QCPE-661).[16] The structures (Figure 1) were plotted by the program AIM 2000.[17] The gradient paths of the electronic density of a point on the IRC path of INCX → IXCN (X = O, S, and Se) (Figures 3−5) were plotted by the GTA-91 program.

3. Results and Discussion

3.1. Potential Energy Curves on IRC Paths. The intrinsic reaction coordinate is defined according to Fukui et al.[18,19] as an imaginary minimum-energy trajectory that passes through the transition state and moves infinitely slowly. Its initial direction at the transition state is given by the normal mode of imaginary frequency. In this work, reaction paths were traced out by the mass-weighted internal coordinate (*S*), which is more precise than a single distance or an angle.[20,21]

Table 1. Optimized Geometry Parameters at the B3LYP/6-311++G(2df) Level[a]

	INCO	INCS	INCSe
B(I−N)	1.9814	1.9704	1.9742
B(N−C)	1.2124	1.2037	1.1997
B(C−X)	1.1629	1.5679	1.7164
A(CNI)	130.2	136.5	137.1
A(XCN)	179.7	174.3	174.8
D(ONCI)	180.0	180.0	180.0
	TS	TS	TS
B(I−N)	3.3355	3.0394	3.0065
B(N−C)	1.2028	1.1843	1.1781
B(C−X)	1.1959	1.6092	1.7642
A(CNI)	60.6	76.7	80.1
A(XCN)	174.0	169.8	169.5
D(XCNI)	0.0	0.0	0.0
	IOCN	ISCN	ISeCN
B(I−X)	2.0209	2.3876	2.5056
B(X−C)	1.2823	1.6867	1.8390
B(C−N)	1.1564	1.1563	1.1550
A(CXI)	119.6	101.3	98.0
A(NCX)	176.2	175.9	177.0
D(NCXI)	180.0	180.0	180.0

[a] B denotes bond length (Å), A denotes bond angle (deg), and D denotes dihedral (deg).

The geometry parameters of reactants, transition states, and products on the potential energy surfaces were optimized and are listed in Table 1. As an example of the series reactions studied, we illustrate the structures of INCS, ISCN, and their transition states in Figure 1. All of the geometries have C_s symmetry; that is, the four atoms are in the same plane in the reactions' paths all along. The geometries of the transition states are found for the first time. The frequencies were computed using the analytical second derivatives to check that the stationary points exhibit the proper number of imaginary frequencies: none for a minimum and one for a transition state (first-order saddle point). IRC calculations were carried out to validate the connection of the transition states to the reactants (INCX) and products (IXCN) (X = O, S, and Se). Along the reaction paths, there is no breakage at the N−C bond or the C−X (X = O, S, and Se) bond, but the I−N bond is broken, and the I−X (X = O, S, and Se) bond forms.

(13) Glukhovtsev, M. N.; Pross, A.; Mcgrath, M. P.; Radom, L. *J. Chem. Phys.* **1995**, *103*, 1878.
(14) Ishida, K.; Morokuma, K.; Komornicki, A. *J. Chem. Phys.* **1977**, *66*, 2153.
(15) Frisch, M. J.; Trucks, G. W.; Schlegel, H. B.; Scuseria, G. E.; Robb, M. A.; Cheeseman, J. R.; Zakrzewski, V. G.; Montgomery, J. A., Jr.; Stratmann, R. E.; Burant, J. C.; Dapprich, S.; Millam, J. M.; Daniels, A. D.; Kudin, K. N.; Strain, M. C.; Farkas, O.; Tomasi, J.; Barone, V.; Cossi, M.; Cammi, R.; Mennucci, B.; Pomelli, C.; Adamo, C.; Clifford, S.; Ochterski, J.; Petersson, G. A.; Ayala, P. Y.; Cui, Q.; Morokuma, K.; Malick, D. K.; Rabuck, A. D.; Raghavachari, K.; Foresman, J. B.; Cioslowski, J.; Ortiz, J. V.; Stefanov, B. B.; Liu, G.; Liashenko, A.; Piskorz, P.; Komaromi, I.; Gomperts, R.; Martin, R. L.; Fox, D. J.; Keith, T.; Al-Laham, M. A.; Peng, C. Y.; Nanayakkara, A.; Gonzalez, C.; Challacombe, M.; Gill, P. M. W.; Johnson, B. G.; Chen, W.; Wong, M. W.; Andres, J. L.; Head-Gordon, M.; Replogle, E. S.; Pople, J. A. *Gaussian 98*, revision A.3; Gaussian, Inc.: Pittsburgh, PA, 1998.
(16) Zheng, S. J.; Cai, X. H.; Meng, L. P. *QCPE Bull.* **1995**, *15*, 25.
(17) Biegler-König, F. *AIM 2000*, version 1.0; University of Applied Science: Bielefeld, Germany, 2000.
(18) Fukui, K.; Kato, S.; Fujimoto, H. *J. Am. Chem. Soc.* **1975**, *97*, 1.
(19) Stanton, R. E.; McIver, J. W., Jr. *J. Am. Chem. Soc.* **1975**, *97*, 3632.
(20) Gonzalez, C.; Schlegel, H. B. *J. Chem. Phys.* **1989**, *90*, 2154.
(21) Gonzalez, C.; Schlegel, H. B. *J. Phys. Chem.* **1990**, *94*, 5523.

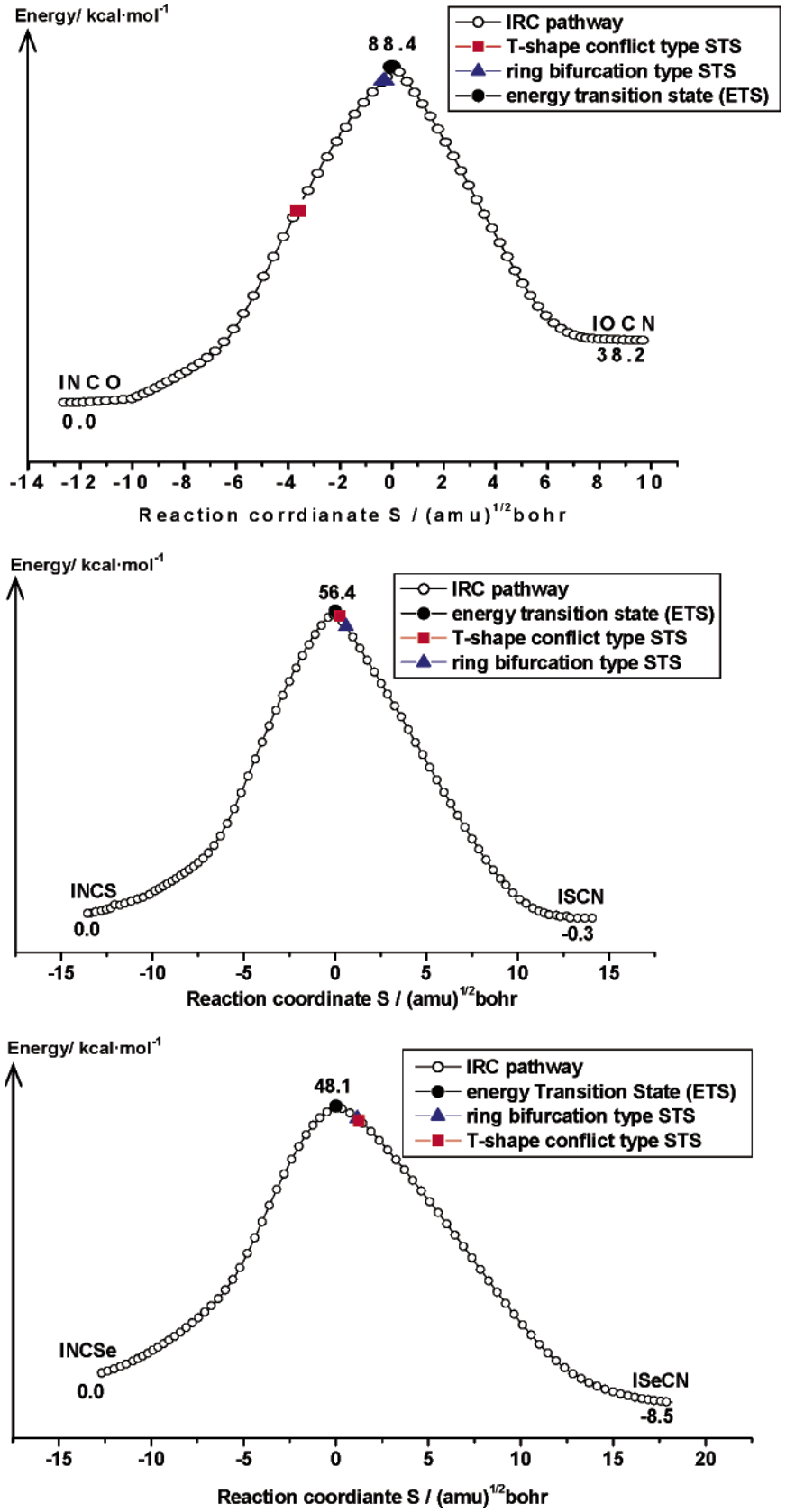

Figure 2. Potential energy curves of the INCX → IXCN (X = O, S, Se) reaction.

The potential energy curves of the titled reactions are given in Figure 2. The process of the reaction INCO → IOCN is endothermic. If the iodine atom is bonded to the OCN group through the O atom, then it is very easy for IOCN to isomerize to INCO. On the contrary, if the iodine atom is bonded to the OCN group through the N atom, it is very difficult for INCO to isomerize to IOCN. Therefore, INCO is detected easily in the experiment. The processes of INCS

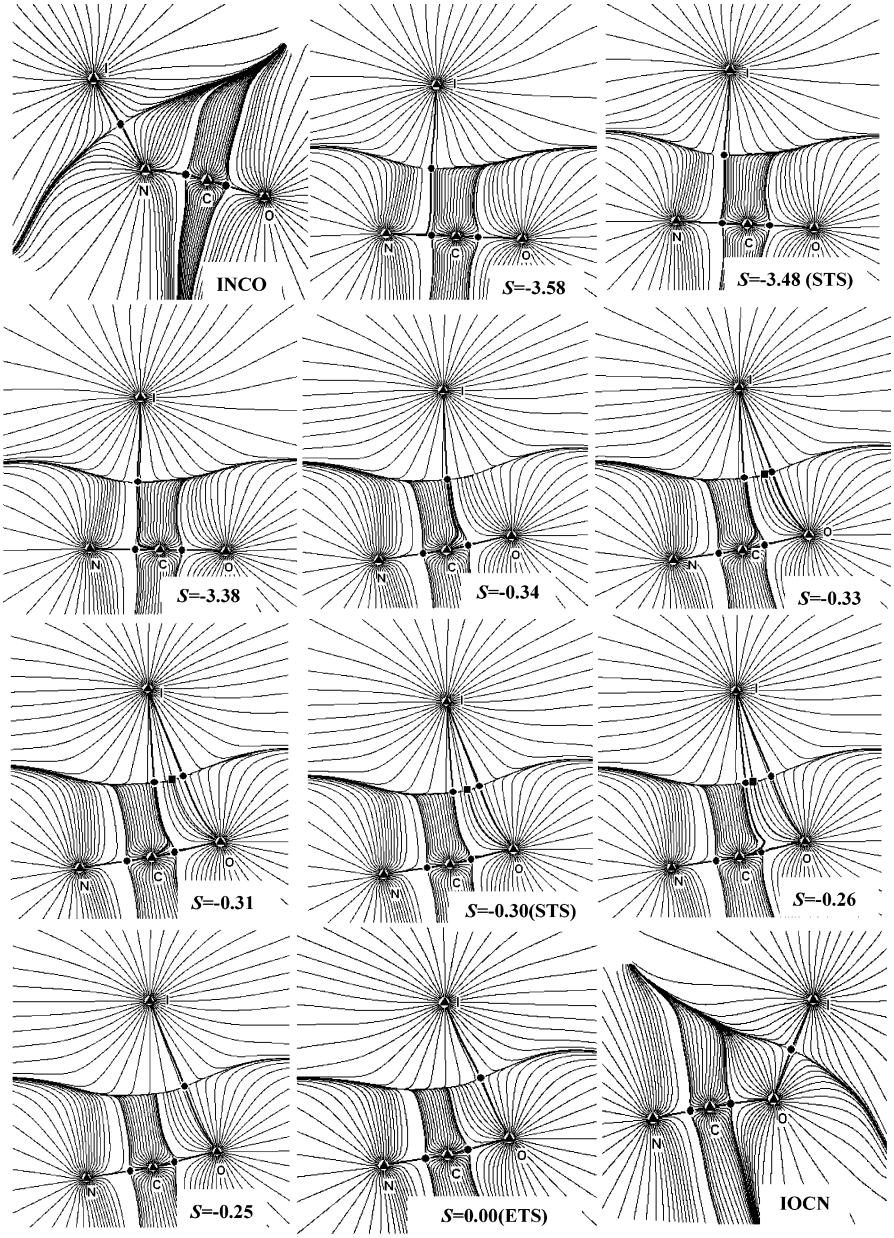

Figure 3. Gradient paths of the electronic density on the IRC path of INCO → IOCN. Triangles denote nuclei, circles denote BCP, and rectangles denote RCP.

→ ISCN and INCSe → ISeCN are exothermic reactions. If the iodine atom is bonded to the SCN or the SeCN group through the S or Se atom, it is very difficult for ISCN and ISeCN to isomerize to INCS and INCSe, respectively. On the contrary, if the iodine atom is bonded to the SCN or the SeCN group through the N atom, it is very easy for INCS and INCSe to isomerize to ISCN and ISeCN, respectively. Therefore, ISCN and ISeCN are detected easily in the experiments.

3.2. Topological Analyses of Electronic Density on IRC Paths. For each reaction, the topological analysis was carried out on the electronic density of every point along the reaction path. Topological properties are listed in Tables 2−4 for INCX → IXCN (X = O, S, and Se), respectively. Gradient paths of the electronic density are plotted for some points along the reaction path and displayed in Figures 3−5 for INCX → IXCN (X = O, S, and Se), respectively.

3.2.1. Changes in Structure Determined by the Topology of the Electron Density. The transition structure on the IRC path for the reaction of A−B−C → B−C−A has been discussed;[22] it is always near the (energy) transition state. In the INCX → IXCN (X = O, S, and Se) process, we still put the emphasis on the narrow area along the reaction path around the (energy) transition state.

According to the topological analysis of electronic density distribution in the AIM,[4,22] $\rho(r_c)$ is used to describe the strength of a bond and $\nabla^2\rho(\boldsymbol{r}_c)$ is used to describe the characteristics of the bond. In general, the larger the value of $\rho(\boldsymbol{r}_c)$, the stronger the bond. The field of $\nabla^2\rho(\boldsymbol{r}_c) < 0$ is a charge-accumulated area, and $\nabla\ ^2\rho(\boldsymbol{r}_c) > 0$ is a charge-dispersed area. $\nabla^2\rho(\boldsymbol{r}_c) = \lambda_1 + \lambda_2 + \lambda_3$, λ_i is an eigenvalue of the Hessian matrix of ρ, and r_c is the critical point (called

(22) Bader, R. F. W. *Chem. Rev.* **1991**, *91*, 1: 893.

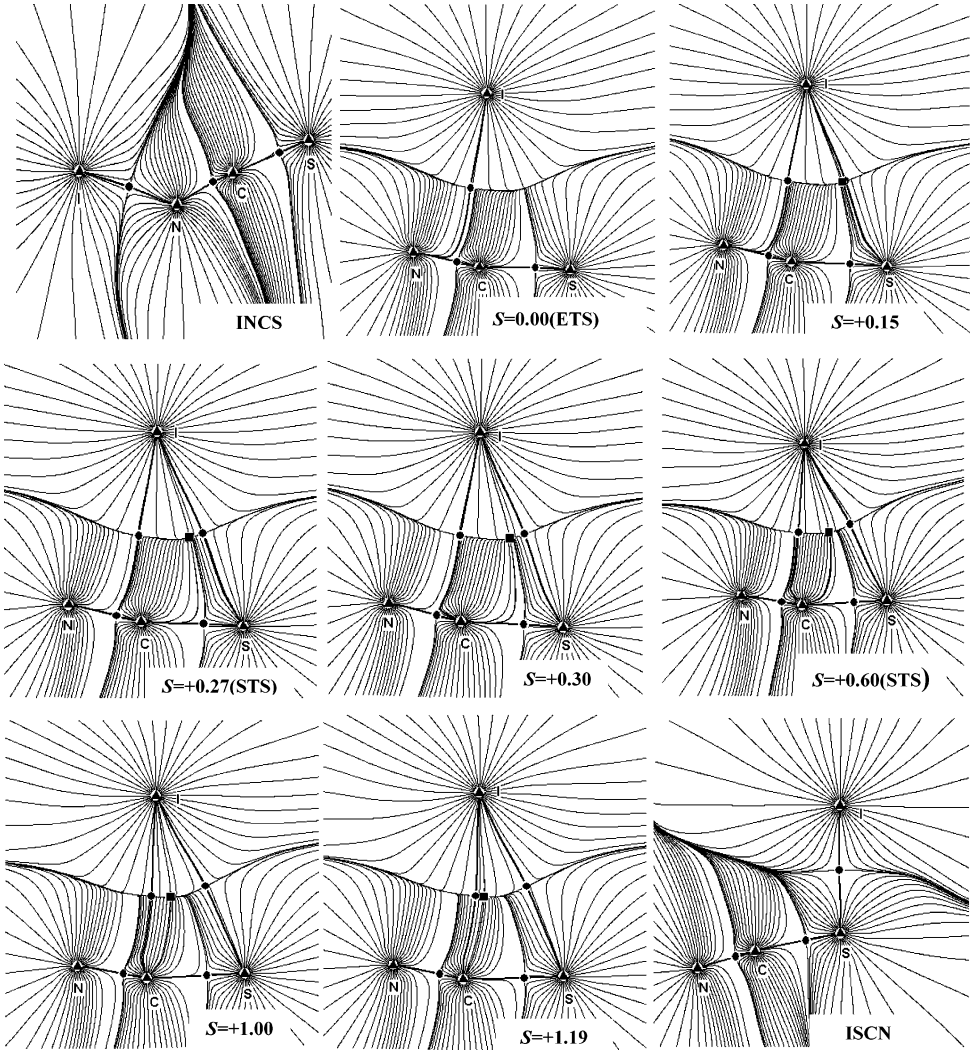

Figure 4. Gradient paths of the electronic density on the IRC path of INCS → ISCN. Triangles denote nuclei, circles denote BCP, and rectangles denote RCP.

a saddle point) on the electronic density surface, which is connected by two gradient paths (called bond paths) forming the bond that connects the two nuclei. Then, when one of the three λ_i is positive and the other two are negative, we denote it by (3, −1) and call it the bond critical point (BCP). When one of the three λ_i is negative and the other two are positive, we denoted it by (3, +1) and call it the ring critical point (RCP), which indicates that a ring structure exists. For the RCP, the single negative curvature (λ_1 in this paper) terminates at the RCP and is thus negative. The density is a minimum in the ring surface at the RCP, and thus the two curvatures (λ_2 and λ_3 in this paper) in the ring surface or plane are positive and originate at the critical point (CP). For the BCP, one negative curvature (λ_1 in this paper) is directed perpendicular to the ring surface, the other negative curvature (λ_2 in this paper) of the BCP lies in the plane of the ring, and the positive curvature (λ_3 in this paper) defines the bond path.

In the INCX → IXCN (X = O, S, and Se) process, the electronic density $\rho(\boldsymbol{r}_c)$ at the BCP of I−N becomes smaller and smaller, which indicates that the I−N bond becomes weaker and weaker, and at last, it is broken. As the reactions proceed, the I−X (X = O, S, and Se) bonds become larger and larger, which indicates that the I−X (X = O, S, and Se) bonds become stronger and stronger, and then IXCN (X = O, S, and Se) comes into being. As the reactions proceed, $\rho(r_c)$ of the BCP of the N−C bond becomes somewhat larger, and $\rho(r_c)$ of the BCP of the C−X (X = O, S, and Se) bond becomes somewhat smaller, which indicates that the N−C bond becomes somewhat stronger, and the C−X (X = O, S, and Se) bond becomes somewhat weaker.

For the INCO → IOCN process, from INCO to the energy transition state (reaction coordinate $S = 0.00$), the I−N bond becomes more and more weak, the bond path becomes more and more bent, and the I−N bond path slides along the N−C bond. At the point $S = -0.48$, there is a bond path between the iodine atom and the BCP of the N−C bond. After that point, the I−C bond formed. Then, the I−C bond path begins to slide along the C−O bond, and the RCP appears at $S = -0.33$. There is an I−C−O three-membered ring in the region of $S = -0.33$ to -0.26. After the point $S = -0.26$, the I−C bond disappears, and the I−O bond becomes stronger and stronger and IOCN forms.

For the INCS → ISCN process, from INCS to the energy transition state, the I−N bond path becomes more and more bent. The RCP appears in the region of $S = +0.15$ to $+1.19$.

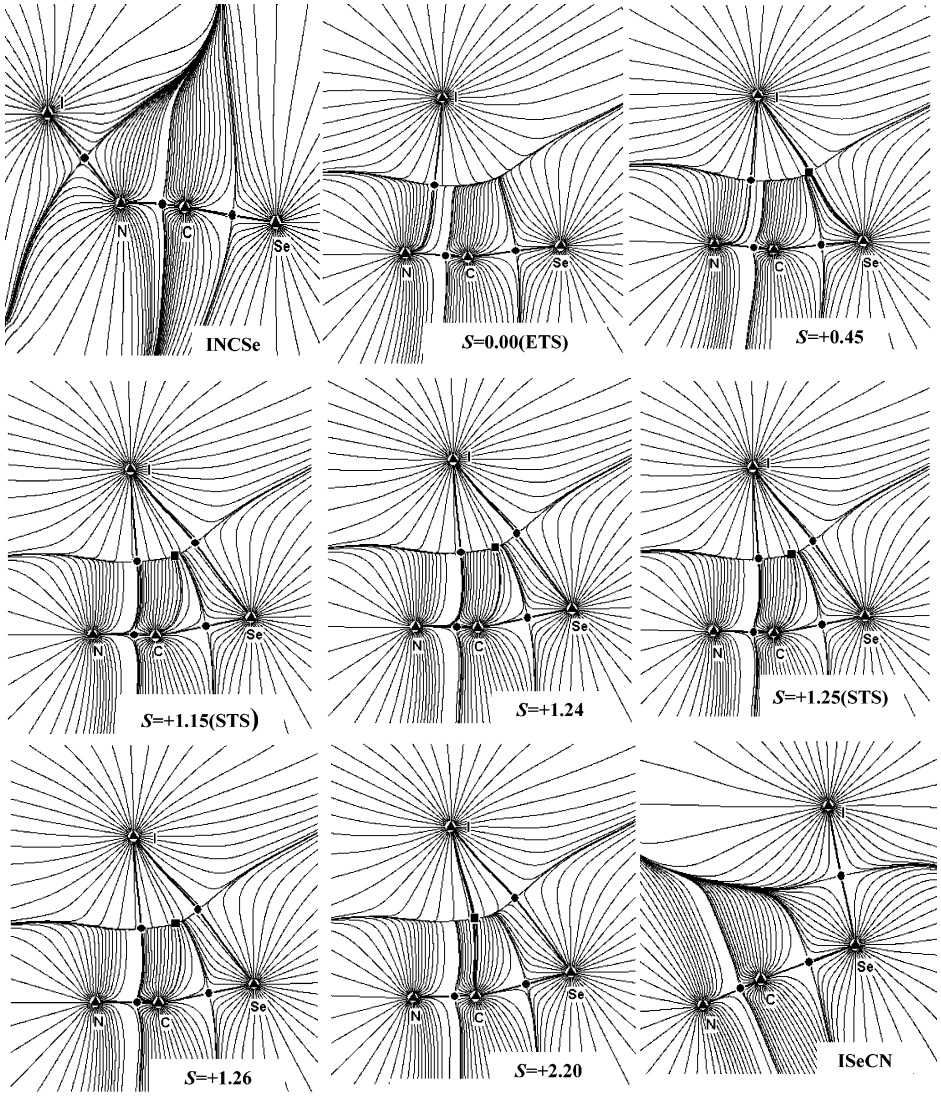

Figure 5. Gradient paths of the electronic density on the IRC path of INCSe → ISeCN. Triangles denote nuclei, circles denote BCP, and rectangles denote RCP.

There is an I−N−C−S four-membered ring in the region of $S = +0.15$ to $+0.27$ and an I−C−S three-membered ring in the region of $S = +0.28$ to $+1.19$. From the energy transition state to the ISCN process, the I−N bond path slides along the N−C bond, there is a bond path between the iodine atom and the BCP of the N−C bond at $S = +0.27$, and the I−C bond comes into being. The I−N−C−S four-membered ring changes to the I−C−S three-membered ring at $S = +0.27$.

For the INCSe → ISeCN process, from INCSe to the energy transition state, the I−N bond path becomes more and more bent. The RCP appears in the region of $S = +0.45$ to $+2.20$. There is an I−N−C−Se four-membered ring in the region of $S = +0.45$ to $+1.25$ and an I−C−Se three-membered ring in the region of $S = +1.26$ to $+2.20$. From the energy transition state to the ISeCN process, the I−N bond path slides along the N−C bond, there is a bond path between the iodine atom and the BCP of the N−C bond at $S = +1.25$, and the I−C bond comes into being. The I−N−C−Se four-membered ring changes to the I−C−Se three-membered ring at $S = +1.25$.

On the basis of the catastrophe theory,[3,4] Bader et al. pointed out that for a simple ABC system a 2D cross section of the structure diagram can be used to predict the existence of conflict-type and bifurcation-type mechanisms.[1−5] In the bifurcation mechanism, the formation or annihilation of the ring structure occurs with the formation of a singularity in the density. At a singularity in the density, the first and second derivatives are zero, and the critical point (CP) has a rank less of than 3; that is, it has a rank of 2 in the present case because there is one zero curvature. The singularity in the density is unstable, and for an infinitesimal increase in the reaction coordinate, it bifurcates into a BCP and an RCP. The negative curvature of the BCP lying in the plane will, like the associated curvature of the RCP, initially be close to zero. Initially, the BCP and RCP will have eigenvectors directed at one another: a positive one for the RCP, and a negative one for the BCP. They increase and decrease, respectively, from zero as the newly formed BCP and RCP separate. As the reaction gets to the point where the BCP and RCP merge, another singularity is formed in the density, the point where a bond is broken. For points very close to

Table 2. Electronic Densities $\rho(r_c)$ at the Critical Points on the INCO → IOCN Pathway and Topologicals Characteristics of the BCP and the RCP of the Ring Transition on the INCO → IOCN Pathway

(a) Electronic Densities $\rho(r_c)$ at the Critical Points on the INCO → IOCN Pathway

$S^{a,b}$	I−N	I−BCP(N−C)	I−C	I−BCP(C−O)	I−O	N−C	C−O
INCO	0.1372					0.4175	0.4440
−3.58	0.0295					0.4147	0.4437
−3.48 (STS)		0.0292				0.4152	0.4429
−3.38			0.0289			0.4151	0.4430
−3.28			0.0286			0.4155	0.4424
−1.89			0.0236			0.4176	0.4395
−0.34			0.0210			0.4278	0.4256
−0.33			0.0210		0.0208	0.4279	0.4252
−0.31			0.0209		0.0208	0.4282	0.4246
−0.30 (STS)				0.0209	0.0209	0.4284	0.4243
−0.25					0.0213	0.4291	0.4228
0.00 (ETS)					0.0232	0.4341	0.4119
IOCN					0.1160	0.4534	0.3358

(b) Topological Characteristics of the BCP and the RCP of the Ring Transition Region on the INCO → IOCN Pathway

			Eigenvalue of the Hessian Matrix			
bond	$S^{a,b}$	ρ	λ_1	λ_2	λ_3	$\nabla^2\rho^c$
I−C	−0.33	0.0210	−0.0134	−0.0036	0.0900	0.0730
	−0.31	0.0209	−0.0134	−0.0032	0.0902	0.0736
	−0.30	0.0209	−0.0134	−0.0028	0.0904	0.0742
	−0.29	0.0209	−0.0134	−0.0024	0.0906	0.0748
	−0.27	0.0209	−0.0134	−0.0025	0.0904	0.0745
	−0.26	0.0209[d]	−0.0134	−0.0014[d]	0.0909	0.0761
I−O	−0.33	0.0207[e]	−0.0128	−0.0019[e]	0.0912	0.0765
	−0.31	0.0208	−0.0129	−0.0028	0.0912	0.0755
	−0.30	0.0209	−0.0130	−0.0033	0.0912	0.0749
	−0.29	0.0210	−0.0130	−0.0036	0.0912	0.0746
	−0.27	0.0212	−0.0133	−0.0051	0.0911	0.0727
	−0.26	0.0213	−0.0131	−0.0044	0.0914	0.0739
RCP	−0.33	0.0207[e]	−0.0130	0.0014[e]	0.0914	0.0798
	−0.31	0.0208	−0.0131	0.0018	0.0913	0.0800
STS	−0.30	0.0208	−0.0131	0.0018	0.0913	0.0800
	−0.27	0.0208	−0.0132	0.0018	0.0915	0.0801
	−0.26	0.0209[d]	−0.0133	0.0012[d]	0.0913	0.0792

[a] S: reaction coordinate in unit of (amu)$^{1/2}$bohr. [b] − denotes reverse direction of the reaction. [c] $\nabla^2\rho$ denotes the Laplacian of electron density. [d] The annihilation of the ring structure with a singularity in the density. [e] The formation of the ring structure with a singularity in the denisty.

the singularity, the two curvatures will have almost equal magnitude and opposite signs.[4]

In the INCS → ISCN process, there is a conflict structure during the migration of the I−N bond to the I−C bond, and a bifurcation-type I−N−C−S ring structure appears in the migration of the iodine atom to form the I−S bond. The formation of the I−N−C−S four-membered ring structure occurs with the formation of a singularity in the density. That is, the density at the newly appearing BCP of the I−S bond and the RCP of the I−N−C−S ring is the same value at the point $S = +0.15$. From Table 3, the λ_2 eigenvalue of the BCP of the I−S bond (the negative curvature lying in the plane) and the associated curvature of the RCP of the I−N−C−S ring structure are close to zero, and they have equal magnitude and opposite signs. In the region of $S = +0.15$ to $+0.60$, the λ_2 eigenvalue of the I−S BCP and the RCP decrease and increase, respectively. After the point $S = +0.60$, the λ_2 eigenvalue of the RCP begins to decrease. As the reaction gets to the point where the BCP of the I−C bond and the RCP merge to form another singularity in the density at the point $S = +1.19$ the I−C bond is broken. (From Table 3, the two curvatures will have almost equal magnitude and opposite signs.) Then, the λ_2 eigenvalue of the BCP of the I−C bond and the associated curvature of the RCP of the I−C−S ring are close to zero.

The INCSe → ISeCN process is similar to the INCS → ISCN process; there is a conflict structure in the migration of the I−N bond to the I−C bond, and a bifurcation-type I−N−C−Se ring structure appears in the migration of the iodine atom to form the I−Se bond. Both the formation of the I−N−C−Se four-membered ring structure and the annihilation of the I−C−Se three-membered ring structure occur with the formation of a singularity in the density (Table 4: $S = +0.45$ for the I−Se BCP and the RCP, $S = +2.20$ for the I−C BCP and the RCP; the two curvatures have almost equal magnitude and opposite signs).

The transition structure of the INCO → IOCN process is different from that of the INCS → ISCN and INCSe → ISeCN processes. In the processes of INCS → ISCN and INCSe → ISeCN, the T-shaped conflict structures ($S = +0.27$ and $+1.25$) are included in the ring structure transition regions ($S = +0.15$ to $+1.19$ and $+0.45$ to $+2.20$), and at these T-shaped conflict structures, the four-membered I−N−C−X ring structures are bifurcated to three-membered I−C−X ring transition structures. Whereas in the INCO → IOCN process the T-shaped conflict structure ($S = -3.48$)

Table 3. Electronic Densities $\rho(r_c)$ at the Critical Points on the INCS → ISCN Pathway and Topological Characteristics of the BCP and the RCP of the Ring Transition Region on the INCS → ISCN Pathway

(a)Electronic Densities $\rho(r_c)$ at the Critical Points on the INCS → ISCN Pathway

$S^{a,b}$	I−N	I−BCP(N−C)	I−C	I−S	N−C	C−S
INCS	0.1395				0.4170	0.2324
0.00(ETS)	0.0203				0.4469	0.2310
+0.15	0.0198			0.0168	0.4489	0.2301
+0.17	0.0197			0.0169	0.4492	0.2300
+0.25	0.0195			0.0171	0.4499	0.2296
+0.27(STS)		0.0194		0.0172	0.4502	0.2295
+0.30			0.0194	0.0173	0.4505	0.2294
+0.40			0.0191	0.0175	0.4515	0.2289
+0.60(STS)			0.0183	0.0184	0.4540	0.2273
+1.00			0.0177	0.0192	0.4558	0.2258
+1.10			0.0175	0.0195	0.4563	0.2253
+1.19			0.0174	0.0197	0.4567	0.2249
+1.20				0.0198	0.4569	0.2247
ISCN				0.0950	0.4600	0.2136

(b) Topological Characteristics of the BCP and the RCP of the Ring Transition Region on the INCS → ISCN Pathway

			Eigenvalue of the Hessian Matrix			
bond	$S^{a,b}$	ρ	λ_1	λ_2	λ_3	$\nabla^2\rho^c$
I−N	+0.15	0.0198	−0.0115	−0.0041	0.0779	0.0623
	+0.17	0.0197	−0.0114	−0.0041	0.0779	0.0624
	+0.25	0.0195	−0.0112	−0.0042	0.0776	0.0622
I−BCP(N−C)	+0.27	0.0194	−0.0112	−0.0042	0.0775	0.0621
I−C	+0.30	0.0194	−0.0111	−0.0042	0.0773	0.0620
	+0.40	0.0191	−0.0109	−0.0042	0.0768	0.0617
	+0.60	0.0183	−0.0103	−0.0039	0.0744	0.0602
	+1.00	0.0177	−0.0099	−0.0029	0.0710	0.0582
	+1.10	0.0175	−0.0098	−0.0022	0.0695	0.0575
	+1.19	0.0174[d]	−0.0097	−0.0014[d]	0.0679	0.0568
I−S	+0.15	0.0168[e]	−0.0083	−0.0009[e]	0.0504	0.0412
	+0.17	0.0169	−0.0082	−0.0016	0.0500	0.0402
	+0.25	0.0171	−0.0084	−0.0031	0.0494	0.0379
	+0.27	0.0172	−0.0084	−0.0034	0.0492	0.0374
	+0.30	0.0173	−0.0085	−0.0037	0.0491	0.0369
	+0.40	0.0175	−0.0087	−0.0048	0.0487	0.0352
	+0.60	0.0184	−0.0093	−0.0069	0.0479	0.0317
	+1.00	0.0192	−0.0099	−0.0085	0.0479	0.0295
	+1.10	0.0195	−0.0102	−0.0089	0.0480	0.0289
	+1.19	0.0197	−0.0103	−0.0092	0.0484	0.0289
RCP	+0.15	0.0168[e]	−0.0084	0.0009[e]	0.0513	0.0438
	+0.17	0.0169	−0.0085	0.0016	0.0517	0.0448
	+0.25	0.0170	−0.0087	0.0030	0.0527	0.0470
	+0.27	0.0171	−0.0087	0.0032	0.0529	0.0474
	+0.30	0.0171	−0.0088	0.0036	0.0532	0.0480
	+0.40	0.0173	−0.0090	0.0043	0.0541	0.0494
	+0.50	0.0174	−0.0092	0.0047	0.0549	0.0504
	+0.55	0.0174	−0.0093	0.0048	0.0554	0.0509
(STS)	+0.60	0.0174	−0.0093	0.0048	0.0559	0.0514
	+0.65	0.0175	−0.0094	0.0048	0.0563	0.0517
	+0.70	0.0175	−0.0095	0.0047	0.0568	0.0520
	+0.80	0.0175	−0.0095	0.0045	0.0578	0.0528
	+0.90	0.0175	−0.0096	0.0041	0.0589	0.0534
	+1.00	0.0175	−0.0097	0.0035	0.0601	0.0539
	+1.10	0.0175	−0.0097	0.0026	0.0617	0.0546
	+1.19	0.0174[d]	−0.0097	0.0015[d]	0.0633	0.0551

[a] S: reaction coordinate in unit of (amu)$^{1/2}$bohr. [b] + denotes forward direction of the reaction. [c] $\nabla^2\rho$: Laplacian of electron density. [d] The annihilation of the ring structure with a singularity in the density. [e] The formation of the ring structure with a singularity in the density.

does not include the ring structure transition region (S = −0.33 to −0.26), it is some distance from the (energy) transition state. The singularities in the density also appear in the formation and annihilation of the I−C−O three-membered ring structure (S = −0.33 for the I−O BCP and RCP, and S = −0.26 for the I−C BCP and RCP).

3.2.2. Structure Transition State and the Structure Transition Region. When a bond is broken and a new bond is formed, the structure transition state and the structure transition region will appear. One is a kind of T-shaped conflict structure transition state that includes a bond path linking a nucleus and a bond critical point (BCP). We call it the first kind of structure transition state. The other one is a kind of bifurcation-type ring structure transition region enveloped by some bond paths and three or more nuclei. As the ring critical point (RCP), appears, it is very close to the

Table 4. Electronic Densities $\rho(r_c)$ at the Critical Points on the INCSe→ ISeCN Pathway and Topological Characteristics of the BCP and the RCP of the Ring Transiton Region on the INCSe → ISeCN Pathway

(a) Electronic Densities $\rho(r_c)$ at the Critical Points on the INCSe→ ISeCN Pathway

$S^{a,b}$	I−N	I−BCP(N−C)	I−C	I−Se	N−C	C−Se
INCSe	0.1405				0.4392	0.2000
0.00(ETS)	0.0214				0.4742	0.1926
+0.45	0.0184			0.0148	0.4540	0.1797
+0.65	0.0178			0.0151	0.4552	0.1786
+1.00	0.0169			0.0157	0.4570	0.1765
+1.10	0.0166			0.0158	0.4575	0.1760
+1.15(STS)	0.0164			0.0159	0.4578	0.1754
+1.24	0.0163			0.0160	0.4579	0.1753
+1.25(STS)		0.0163		0.0160	0.4580	0.1752
+1.26			0.0163	0.0160	0.4581	0.1751
+1.38			0.0160	0.0162	0.4583	0.1745
+1.49			0.0158	0.0164	0.4584	0.1740
+1.70			0.0155	0.0166	0.4589	0.1731
+1.90			0.0152	0.0169	0.4591	0.1725
+2.10			0.0150	0.0171	0.4594	0.1718
+2.20			0.0149	0.0172	0.4595	0.1715
ISeCN				0.0879	0.4886	0.1719

(b) Topological Characteristics of the BCP and the RCP of the Ring transition Region on the INCSe → ISeCN Pathway

			Eigenvalue of the Hessian Matrix			
bond	$S^{a,b}$	ρ	λ_1	λ_2	λ_3	$\nabla^2\rho^c$
I−N	+0.45	0.0184	−0.0103	−0.0021	0.0712	0.0588
	+0.65	0.0178	−0.0098	−0.0023	0.0699	0.0578
	+1.00	0.0169	−0.0091	−0.0028	0.0667	0.0548
	+1.10	0.0166	−0.0089	−0.0028	0.0657	0.0540
	+1.15	0.0164	−0.0087	−0.0028	0.0647	0.0532
	+1.24	0.0163	−0.0087	−0.0028	0.0642	0.0527
I−BCP(N−C)	+1.25	0.0163	−0.0087	−0.0028	0.0641	0.0526
I−C	+1.26	0.0163	−0.0086	−0.0028	0.0640	0.0526
	+1.49	0.0158	−0.0083	−0.0027	0.0614	0.0504
	+1.70	0.0155	−0.0081	−0.0025	0.0591	0.0485
	+1.90	0.0152	−0.0079	−0.0020	0.0568	0.0469
	+2.10	0.0150	−0.0077	−0.0013	0.0541	0.0451
	+2.20	0.0149[d]	−0.0076	−0.0002[d]	0.0513	0.0435
I−Se	+0.45	0.0148[e]	−0.0064	−0.0005[e]	0.0374	0.0305
	+0.65	0.0151	−0.0065	−0.0030	0.0359	0.0264
	+1.00	0.0157	−0.0069	−0.0048	0.0349	0.0232
	+1.10	0.0158	−0.0070	−0.0051	0.0347	0.0226
	+1.15	0.0159	−0.0071	−0.0054	0.0346	0.0221
	+1.24	0.0160	−0.0071	−0.0055	0.0345	0.0219
	+1.25	0.0160	−0.0071	−0.0056	0.0345	0.0218
	+1.26	0.0160	−0.0072	−0.0055	0.0345	0.0218
	+1.49	0.0164	−0.0074	−0.0062	0.0342	0.0206
	+1.70	0.0166	−0.0076	−0.0067	0.0344	0.0201
	+1.90	0.0169	−0.0078	−0.0070	0.0346	0.0198
	+2.10	0.0171	−0.0079	−0.0074	0.0350	0.0197
	+2.20	0.0172	−0.0080	−0.0076	0.0352	0.0196
RCP	+0.45	0.0148[e]	−0.0064	0.0005[e]	0.0379	0.0320
	+0.65	0.0150	−0.0068	0.0031	0.0391	0.0354
	+1.00	0.0152	−0.0072	0.0043	0.0404	0.0375
	+1.05	0.0152	−0.0072	0.0043	0.0406	0.0377
	+1.10	0.0152	−0.0072	0.0044	0.0408	0.0380
(STS)	+1.15	0.0152	−0.0072	0.0044	0.0410	0.0382
	+1.20	0.0152	−0.0073	0.0044	0.0413	0.0384
	+1.25	0.0152	−0.0073	0.0044	0.0415	0.0386
	+1.29	0.0152	−0.0073	0.0043	0.0416	0.0386
	+1.49	0.0152	−0.0074	0.0039	0.0430	0.0395
	+1.70	0.0152	−0.0075	0.0034	0.0443	0.0402
	+1.90	0.0151	−0.0075	0.0026	0.0459	0.0410
	+2.10	0.0150	−0.0076	0.0015	0.0480	0.0419
	+2.20	0.0149[d]	−0.0076	0.0002[d]	0.0506	0.0432

[a] S: reaction coordinate in unit of (amu)$^{1/2}$bohr. [b] + denotes forward direction of the reaction. [c] $\nabla^2\rho$ is the Laplacian of electron density. [d] The annihilation of the ring structure with a singularity in the density. [e] The formation of the ring structure with a singularity in the density.

BCP of the newly formed bond. As the process proceeds, the RCP moves to the center of the ring. When the RCP goes near the BCP of another bond, this bond is broken, and the ring disappears. From the ring's appearance to its disappearance, the λ_2 eigenvalue of the Hessian matrix of the RCP (the positive curvature lying in the plane) has the trends of zero (close to zero) to maximum to zero (close to zero). We define the point corresponding to the maximum

of the Hessian matrix λ_2 value as the second kind of structure transition state of the bifurcation-type ring structure transition region. We call the T-shaped conflict-type transitional structure or bifurcation-type ring transitional structure a structure transition state (STS). For clarity, the traditional transitional state that is the maximum on the energy surface is called the energy transition state (ETS).

Both kinds of structure transition states appear in the INCX → IXCN (X = O, S, and Se) process. We observed that at $S = -3.48$ for the INCO → IOCN process, $S = +0.27$ for the INCO → IOCN process, and $S = +1.25$ for the INCSe → ISeCN process all are T-shaped conflict STSs. There is a bifurcation-type ring structure transition region for each of the INCX → IXCN (X = O, S, and Se) processes: $S = -0.33$ to -0.26, $+0.15$ to $+1.19$, and $+0.45$ to $+2.20$. The bifurcation-type STS of the structure transition regions are $S = -0.30$, $+0.60$, and $+1.15$ for the INCX → IXCN (X = O, S, and Se) processes, respectively.

Figure 2 also gives the position of the STS and ETS along the reaction pathways. The process of INCO → IOCN is endothermic, and the T-shaped conflict STS ($S = -3.48$) and bifurcation-type ring STS ($S = -0.30$) appear before the ETS ($S = 0.00$). The INCS → ISCN process is exothermic, and the T-shaped STS ($S = +0.27$) and the ring STS ($S = +0.60$) appear after the ETS ($S = 0.00$). The INCSe → ISeCN process is an exothermic reaction, and the T-shaped STS ($S = +1.25$) and the ring STS ($S = +1.15$) appear after the ETS ($S = 0.00$). These are in accordance with the conclusion that the "STS state appears before ETS in endothermic reactions, STS appears after ETS in exothermic reactions".[23−25]

The positions of the STSs are $S = -3.48$ and -0.30, $S = +0.27$ and $+0.60$, and $S = +1.25$ and $+1.15$ for the INCX → IXCN (X = O, S, and Se) processes, respectively. That is, the position of the STS appears later and later according to the sequence of O, S, and Se. The ranges of the ring structure regions are $S = -0.33$ to -0.26, $S = +0.15$ to $+1.19$, and $S = +0.45$ to $+2.20$ for the INCX → IXCN (X = O, S, and Se) processes, respectively. That is, the ranges of the ring structure regions become wider and wider according to the sequence of O, S, and Se. The sulfur and selenium atoms have much larger van der Waals and covalent radii than oxygen, which can explain the sequence of the width of the ring structure transition regions.

4. Conclusions

(1) The geometries of the transition states of the topic reactions are reported for the first time. The process of INCO → IOCN is difficult, and the reverse process is easy; the processes of INCX → IXCN (X = S and Se) are easy, and the reverse processes are difficult. Therefore, INCO, ISCN, and ISeCN are more easily detected than IOCN, INCS, and INCSe, respectively.

(2) There are two kinds of STS in the topic reactions: the T-shaped conflict STS and the three- or four-membered ring STS. In the ring structure transition region, from the ring's appearance to its disappearance, the λ_2 eigenvalue of the Hessian matrix of the RCP (the positive curvature lying in the plane) has the trend of zero → maximum → zero. We define the point corresponding to the maximum of the Hessian matrix λ_2 value as the second kind of structure transition state of the bifurcation-type ring transition region.

(3) The process of INCO → IOCN is endothermic, the T-shaped STS and ring STS appear before the ETS, INCX → IXCN (X = O and Se) processes are exothermic, the T-shaped STS and the ring STS appear after the ETS, which is in accordance with the conclusion that the "STS state appears before ETS in endothermic reactions, STS appears after ETS in exothermic reactions".

(4) The position of the STS on the IRC path changed according to the sequence of O, S, and Se, and the ranges of the ring structure regions were also consistent with the sequence of O, S, and Se.

Acknowledgment. This project was supported by the Nature Science Foundation of Hebei Province (contract no. B2004000147). Y.Z. thanks the Chinese Academy of Sciences for a scholarship during the period of this work.

IC0496121

(23) Zheng, S. J.; Meng, L. P.; Cai, X. H.; Xu, Z. F.; Fu, X. Y. *J. Comput. Chem.* **1997**, *18*, 1167.
(24) Zeng, Y. L.; Meng, L. P.; Zheng, S. J. *Acta Chim. Sin. (Chin. Ed.)* **2001**, *59*, 56.
(25) Zeng, Y. L. M.S. Thesis, Hebei Normal University, Shijiazhuang, P. R. China, 2000.